

Bismuth cuprate high- T_c superconductors using cationic substitution

J.-M. Tarascon, P. Barboux, and G. W. Hull
Bellcore, Red Bank, New Jersey 07701

R. Ramesh
National Center for Electron Microscopy, Lawrence Berkeley Laboratory, Berkeley, California 94720

L. H. Greene and M. Giroud
Bellcore, Red Bank, New Jersey 07701

M. S. Hegde
Center for Ceramics Research, Rutgers University, Piscataway, New Jersey 08854

W. R. McKinnon
National Research Council, Division of Chemistry, Ottawa, Canada K1A0R9
(Received 12 October 1988)

The $\text{Bi}_4\text{Sr}_4\text{Ca}_{2-x}\text{R}_x\text{Cu}_4\text{O}_y$ materials (R is a rare-earth element) were studied to determine their structural and physical properties. For most of the rare-earth elements, a complete solid solution exists up to $x=2$. Below $x=0.5$, T_c is not affected and for each added rare-earth element we find that about 0.5 oxygen atom is added to the structure. However, the structural modulation observed along the b axis for the undoped material persists and remains of the same amplitude for the rare-earth-doped samples. When more than one R ($x \geq 1$) is substituted, T_c is depressed and the compound becomes semiconducting beyond $x=1.5$. The depression in T_c from 85 K ($x=0$) to less than 4.2 K ($x=1.5$) correlates to a decrease in the formal valence of copper and is independent whether the rare-earth element is magnetic or nonmagnetic. No evidence for magnetic ordering over the range of temperature 1.7–400 K has been observed in all the substituted compounds. The substitution for Cu by $3d$ metals or for Sr by rare-earth elements fails for the 85-K Bi phase but succeeds for the 10-K Bi phase. Consequently, the following series $\text{Bi}_2\text{Sr}_2\text{Cu}_{1-x}\text{M}_x\text{O}_y$ ($M=\text{Fe}, \text{Co}$) and $\text{Bi}_2\text{RCaCuO}_y$ ($R=\text{La}, \text{Pr}, \text{Nd}, \text{Sm}$) were made for study. These substitutions result in an uptake of oxygen (0.5 for each substituted element). But the materials become semiconducting even though the formal valence of Cu remains greater than 2. An antiferromagnetic transition at 140 K has been found for the Co sample.

I. INTRODUCTION

After two years of intensive research on the high- T_c copper oxides, the mechanism for superconductivity in these materials still remains to be determined. However, the study of new materials and chemically substituted phases has revealed several important trends in properties and this may contribute to the developments of a viable theory. In these materials, the formal valence of copper (between 2 and 3) is one of the crucial parameters for the occurrence of superconductivity. Changing the Cu valence can be achieved by cationic substitutions as in $\text{La}_{2-x}\text{Sr}_x\text{CuO}_4$ (Refs. 1–4) (denoted as the 40-K phase) or by modification of the oxygen content as in $\text{YBa}_2\text{Cu}_3\text{O}_{7-y}$ (Refs. 5 and 6) (denoted as the 90-K phase). For both systems, it was found that T_c increases with increasing the amount of Cu III that is commonly associated with the number of holes. However, in the 40-K phase there is a threshold value, beyond which T_c decreases.^{1,3} Another common feature for these cuprates, whose structure consists of a packing of CuO_2 layers separated by ionic-type sheets, is their low dimensionality

resulting in anisotropic physical properties. From a comparison of the 40- and 90-K phases it was suggested that one-dimensional (1D) linear CuO chains were required to obtain higher- T_c materials. But with the discovery of superconductivity above 85 K for several Bi (Refs. 7–10) and Tl (Ref. 11) oxide phases the need for Cu-O chains was unambiguously ruled out. Finally, both the 40- and 90-K phases have closely related “parent” compounds [such as La_2CuO_4 (Ref. 12) and $\text{YBa}_2\text{Cu}_3\text{O}_6$ (Ref. 13)] that are antiferromagnetic insulators. Based on these experimental facts and on several theoretical calculations, it has been proposed by several authors that magnetic interactions may enhance the pairing of the superconducting electrons.^{14–16}

The discovery of the Bi-based materials provided another opportunity to test the above trends dealing with copper valence, low dimensionality, and magnetism. Since chemical substitutions have already turned out to be of great help in enhancing our understanding of the 40- (Ref. 17) and 90-K (Refs. 18–20) phases, we extended these studies to the Bi systems. Three phases of general formula $\text{Bi}_2\text{Sr}_2\text{Ca}_{n-1}\text{Cu}_n\text{O}_y$ with $n=1, 2,$ and 3 and T_c 's of re-

spectively 10,^{21,22} 85,⁸⁻¹⁰ and 110 K (Refs. 23 and 24) have been isolated in the Bi system. In the following we will name the Bi phases after their number of Bi, Sr, Ca, and Cu atoms per formula unit so that, for example, the $\text{Bi}_4\text{Sr}_3\text{Ca}_3\text{Cu}_4\text{O}_y$ and $\text{Bi}_2\text{Sr}_2\text{Cu}_2\text{O}_y$ will be denoted as 4:3:3:4 and 2:2:0:1, respectively. The research results reported in this paper are concerned mainly with the 85-K phase which is the easiest to make as a pure phase. However, some results for the closely related 2:2:0:1 phase will be described. With the Bi phase, in contrast to the 90-K material, the destruction of T_c via changes in oxygen content is not achievable without destroying the structure.^{8,24} Thus, because of the difficulties encountered in removing oxygen from these materials, we were left only with cationic substitution as a variable in monitoring T_c in the Bi-based compounds as a function of the composition.

The pseudotetragonal substructure of the 85-K Bi phase of ideal composition 4:4:2:4 can be viewed as a three-dimensional packing of $\text{Bi}_2\text{Sr}_2\text{CaCu}_2\text{O}_y$ slabs along the c axis with the main feature being the presence of crystallographically sheared BiO layers separated by a quite long distance of 3.0 Å. Because of the presence of a structural modulation along the b axis, the real structure is not fully determined. There are several unanswered key questions. For example, it is actually not possible to prepare the 4:4:2:4 composition as a single phase by solid-state reactions. In fact, a single phase is formed in the composition range $\text{Bi}_4\text{Sr}_{4-2z}\text{Ca}_{2+z}\text{Cu}_4\text{O}_{16+y}$, only with $0.5 < z < 2.0$.²⁵ This means that Ca and Sr are mixed within their respective sites. The formula should therefore be written $\text{Bi}_4(\text{Sr,Ca})_4(\text{Ca,Sr})_2\text{Cu}_4\text{O}_{16+y}$. The value of y is around 0.3 and the location of these extra oxygen atoms has not yet been unambiguously determined, although simple considerations on the structure have placed them between the Bi-O layers.⁸ Also, the origin of the strong structural modulation^{9,26,27} along the b axis, detectable even by x rays, remains to be clarified. It has been argued that it is associated to the displacement of the Bi atoms in the (a,c) plane.^{26,27} However, the role of the oxygen stoichiometry on this modulation remains to be defined. Thus, any cationic substitution able to modify the oxygen content in this Bi phase should shed some light on the above questions.

As a guide to selecting (based on the steric factors only) the kind of cationic substitution that should have any chance of success for the Bi phases, we compare, in Fig. 1, the substructure of the 85-K Bi-based materials with those of the 40- and 90-K phases (by substructure, we mean the simplest and smallest cell that ignores the modulation mentioned above). The following substitutions were tried.

(i) A remarkable similarity between the Bi and the 90-K structure is that Ca and Y occupy identical crystallographic sites [sharing edges with eight CuO_5 pyramids and faces with two Sr (Ba) polyhedra], suggesting that within the Bi phase Ca may be replaced by Y (as was already shown²⁸⁻³⁰) or by the rare-earth elements as shown herein.

(ii) The crystallographic site of Sr in the Bi phase is similar to that of Ba in the 90-K or that of La in the 40-K phase (ninefold coordinated). Therefore, by analogy to

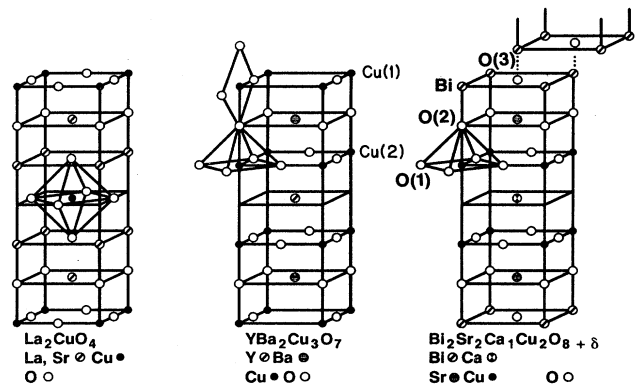


FIG. 1. Crystal structures of (a) La_2CuO_4 , (b) $\text{YBa}_2\text{Cu}_3\text{O}_{7-y}$, and (c) $\text{Bi}_4\text{Sr}_4\text{Ca}_2\text{Cu}_4\text{O}_{16+y}$.

the substitution of La by Sr in the 40-K phase or of Ba by Sr in the 90-K phase,³¹ we attempted the replacement of Sr by rare-earth elements in the Bi phase.

(iii) Among these cuprate phases it is believed that superconductivity resides in the CuO_2 planes and so far substitution for Cu in these planes, either within the 40- or the 90-K phases, have led to a drastic decrease in T_c . Thus, we looked for the same effect within the new Bi phases.

In this paper we first report separately the chemical substitutions on either Cu, Sr, or Ca sites, and their effects on the structural, chemical, and physical properties of the resulting materials. We then discuss the results as related to the large amount of data already existing in the literature for the cuprate oxides.

II. RESULTS

A. Substitution for Ca

Because of the possible mixing of Sr and Ca in their respective sites, two series of samples of nominal composition $\text{Bi}_4\text{Sr}_4\text{Ca}_{2-x}\text{R}_x\text{Cu}_4\text{O}_{16+y}$ (referred to as 4:4:2:4 samples) and $\text{Bi}_4\text{Sr}_3\text{Ca}_{3-x}\text{R}_x\text{Cu}_4\text{O}_{16+y}$ (referred to as 4:3:3:4 samples) with both a magnetic rare earth (Tm) and a nonmagnetic one (Lu) were prepared and studied. The samples were prepared by first heating a mixture containing stoichiometric amounts of Ca and Sr carbonates and of Bi, Cu, and rare-earth oxides. The resulting materials were ground and reannealed several times prior to being pressed into pellets for physical measurements. The heating treatments were performed in an ambient atmosphere and the samples were usually cooled down to room temperature in approximately 6 h. The annealing temperature required to obtain single-phase materials with $M = \text{Tm}$ or Lu was found to be 40°C higher for the 4:4:2:4 than for the 4:3:3:4 series (900°C instead of 860°C). Single-phase materials (as determined by x rays) were obtained only for values of x lower than 2.0 for the 4:3:3:4 series as well as for the 4:4:2:4 samples. This means that Ca can be fully replaced in the 4:4:2:4 compositions, whereas it is not the case in the 4:3:3:4 material.

Substitution is then limited to the Ca site only.

The variation of the lattice parameters for the 4:4:2:4 and 4:3:3:4 series as a function of x were identical for both Tm and Lu. Thus, we show in Fig. 2 the data for the thulium series only. Independent of the starting nominal compositions, 4:4:2:4 or 4:3:3:4, the lattice parameters are changing in a similar manner as a function of the composition. The a axis is going through a minimum, whereas the c axis and the unit-cell volume (V) decrease continuously. The unit-cell volume is higher for the 4:4:2:4 than for the 4:3:3:4 series, as expected, since we have a larger ratio of [Sr]/[Ca] and that Sr^{2+} is larger than Ca^{2+} . This is consistent with a previous study of the $\text{Bi}_4\text{Sr}_{3+x}\text{Ca}_{3-x}\text{Cu}_4\text{O}_y$ series which shows that V increases with increasing x .²⁵ Upon increasing the Tm content, the lattice parameters for both series converge.

High-resolution transmission electron microscopy (HREM) along with energy dispersive x-ray microanalysis, shows that Tm has replaced Ca in the unit cell. One typical image in the [010] zone-axis orientation is shown in Fig. 3(a). Observation of the crystal in the [100] zone-axis orientation [Fig. 3(b)] also shows that the incommensurate modulation of the structure is still present in the phase. The inset in this figure shows the [100] zone-axis selected-area diffraction (SAD) pattern. This SAD pattern is similar to the one of an undoped material, suggesting that the replacement of Ca by Tm (and the consequent introduction of oxygen for charge balance) does not change the nature of the incommensurate modulation although it is slightly decreased from 4.7*b* to 4.3*b*.

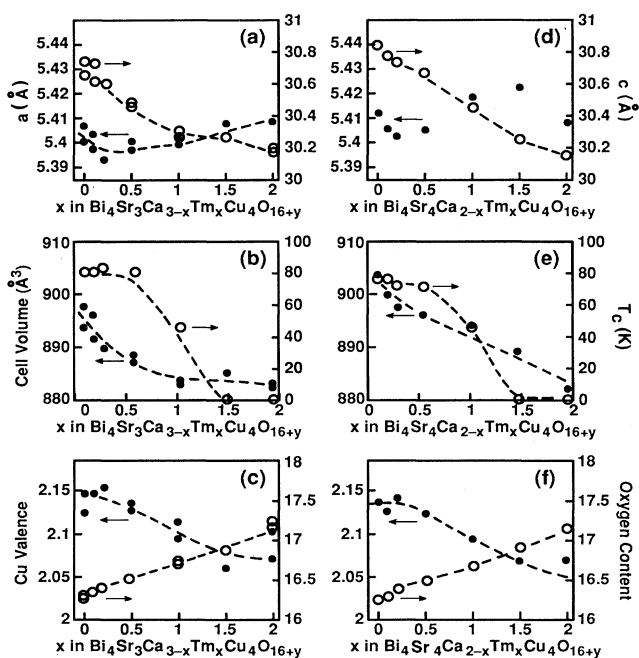


FIG. 2. (a),(d) the lattice parameters; (b),(e) cell volume and T_c ; (c),(f) copper valence and oxygen content are shown for the $\text{Bi}_4\text{Sr}_3\text{Ca}_{3-x}\text{Tm}_x\text{Cu}_4\text{O}_{16+y}$ and $\text{Bi}_4\text{Sr}_4\text{Ca}_{2-x}\text{Tm}_x\text{Cu}_4\text{O}_{16+y}$ series. The dashed lines, joining the experimental points, are just guides for the reader.

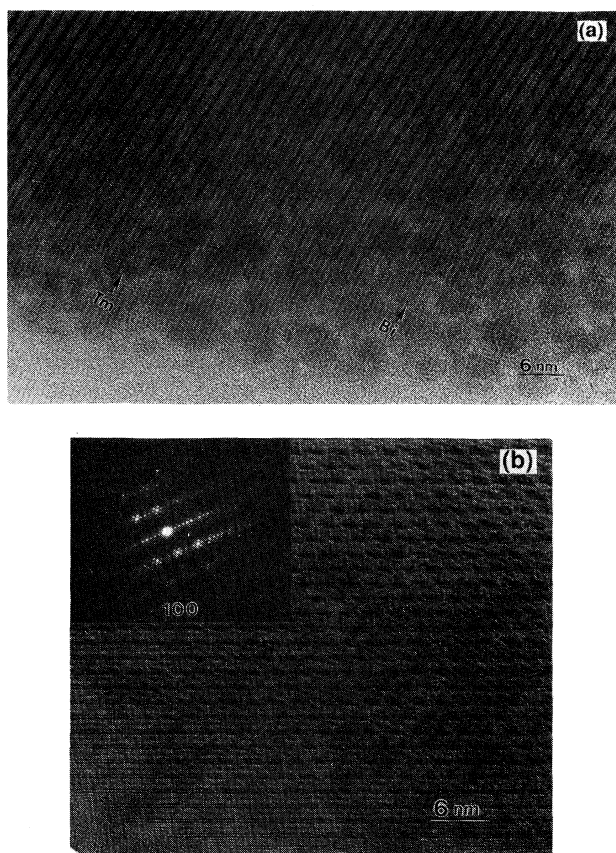


FIG. 3. High resolution electron microscopy image (a) in the [010] zone axis showing the Bi layers and the prominent Tm layers (arrowed). (b) In the [100] zone axis showing the modulated structure similar to that in undoped $\text{Bi}_4\text{Sr}_4\text{Ca}_2\text{Cu}_4\text{O}_{16}$ samples. Inset shows the [100] selected area diffraction pattern.

A detailed analysis of the HREM images will be published separately.

In the light of the above result, attempts were made to prepare the series of compounds $\text{Bi}_4\text{Sr}_4\text{R}_2\text{Cu}_4\text{O}_y$, with R being the rare-earth elements. We found that all the phases do form, but, samples with the rare-earth end members (La, Pr on one side, Yb and Lu on the other) were always contaminated by impurity phases as determined by x-ray diffraction. For the largest rare-earth element single-phase materials were more easily obtained by using Ca instead of Sr (i.e., $\text{Bi}_4\text{Ca}_4\text{La}_2\text{Cu}_4\text{O}_y$). The annealing temperatures required to obtain single-phase materials are different for each of the rare-earth elements, with the highest one (960 °C) being for the lightest rare-earth elements (Pr, La), and the lowest one (900 °C) being for the heaviest rare-earth elements (Lu, Yb). The temperature range at which the rare-earth-doped 4:4:2:4 phase forms is narrow (about 60 °C) usually with a contamination by the $\text{Bi}_2\text{Sr}_2\text{Cu}_4\text{O}_6$ phase at too low or too high temperatures. The Er-doped 4:4:2:4 phase was the easiest one to form cleanly, leading to well-crystallized powders as indicated in the x-ray powder-diffraction pattern in Fig. 4(a). Displayed along with this is the x-ray

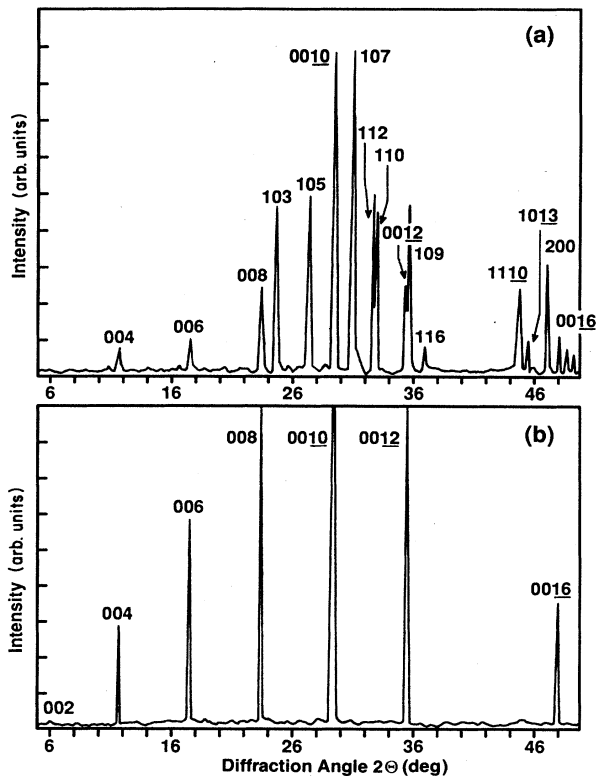


FIG. 4. X-ray powder-diffraction pattern of the $\text{Bi}_4\text{Sr}_4\text{Er}_2\text{Cu}_4\text{O}_{16+y}$. The pattern of a polycrystalline powder is shown in (a) with the Miller indexes noted above each peak. The x-ray diffraction pattern is shown also for highly c -oriented crystals of the same phase in (b).

pattern of plateletlike crystals of the same phase grown using Bi_2O_3 , in excess, as a flux [Fig. 4(b)]. The crystals were pressed onto a glass slide, and because of the strong preferential orientation only the (001) planes are observed. Figures 5(a) and 5(b) show the variation of the a axis and the unit-cell volume for the rare-earth series. The a -axis lattice parameter increases continuously and then saturates for the largest ions (La,Pr), while V increases continuously throughout the rare-earth series (i.e., as the size of the rare-earth ion increases). The monotonic increase suggests that all the rare-earth elements adopt the valence +3 in these materials. The difficulty in preparing the end members of the rare-earth series while the phases from Tm to Nd are easily prepared is reminiscent of similar results found within the $\text{RBa}_2\text{Cu}_3\text{O}_{7-x}$ series in which the compounds with La and Pr or Lu and Yb are difficult to obtain as well. The analogy is not surprising since in both systems the crystallographic site occupied by the rare-earth elements is similar. Finally, it is interesting to note that the Bi-phase doped with Tb can be made while the synthesis of the $\text{TbBa}_2\text{Cu}_3\text{O}_y$ (90-K phase) remains unachievable.

There remains in the Bi system a third phase, the $\text{Bi}_2\text{Sr}_2\text{Ca}_2\text{Cu}_3\text{O}_y$ ($n=3$) phase, which differs structurally from the $n=2$ phase by an extra CaCuO_2 sandwich, but there has been several difficulties in isolating this phase.

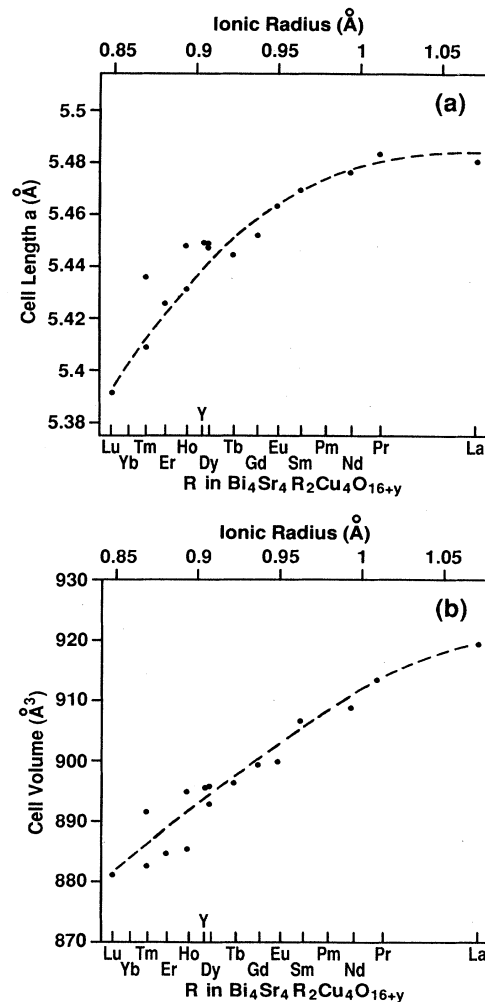


FIG. 5. The variation of the unit-cell parameters " a " and " V " for the $\text{Bi}_4\text{Sr}_4\text{R}_2\text{Cu}_4\text{O}_{16+y}$ series (R = all the rare earth elements) are shown in (a) and (b), respectively. They are plotted as a function of their ionic radii taken from Shannon-Prewitt tables, in the coordinance VI (the only one with a complete set of data).

We tried to prepare this $n=3$ phase with the rare-earth elements instead of Ca but never succeeded in obtaining traces of this phase regardless of the preparation temperature and processing.

The substitution of divalent Ca by trivalent rare-earth elements is expected to either modify the copper valence or to pull into the structure some oxygen or both, in order to maintain charge neutrality. The oxygen contents for the 4:4:2:4 and 4:3:3:4 Tm series (determined by chemical analysis), are shown in Figs. 2(c) and 2(f) along with the Cu valence. We note a continuous increase in oxygen content from 16.2 to 17.3 per formula unit upon increasing the rare-earth content from 0 to 2. This indicates that for each added rare-earth element, half an oxygen atom is added to the structure. Within the same composition range, we note that the Cu valence is constant up to $x=0.5$ and then decreases but still remains greater than 2

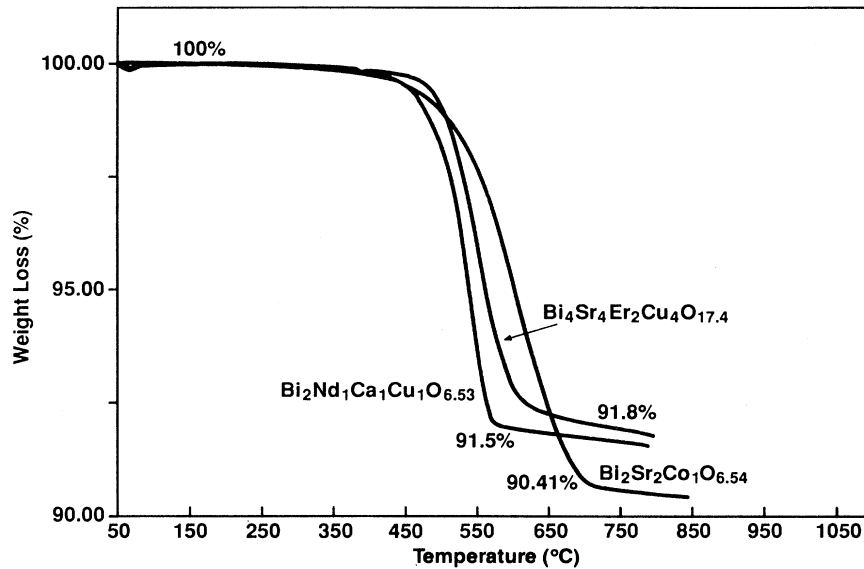


FIG. 6. TGA traces showing the weight loss of the $\text{Bi}_4\text{Sr}_4\text{Er}_2\text{Cu}_4\text{O}_y$, $\text{Bi}_2\text{NdCaCuO}_y$, and $\text{Bi}_2\text{Sr}_2\text{CoO}_y$ when heated up to 850°C at a rate of $10^\circ\text{C}/\text{min}$ under a reducing Ar/H_2 mixture.

for $x=2$. The Cu valence and then the oxygen content have been measured for the $\text{Bi}_4\text{Sr}_4\text{Ca}_{2-x}\text{R}_x\text{Cu}_4\text{O}_{16+y}$ ($x=0.5, 1.0, 1.5$, and 2) series using both thermogravimetry analysis measurements (TGA) under a reducing atmosphere ($\text{Ar}-\text{H}_2$ mixture) and chemical techniques. The values for oxygen content determined by TGA are higher than those obtained from chemical analysis. For instance, an oxygen content of 17.5 per formula unit was found by TGA for the Er phase (Fig. 6), while chemical titration gives only 17.3. However, although quite different, both results agree to show that the copper valence remains above two upon rare-earth substitution. The copper and oxygen contents (as determined chemically) are plotted in Fig. 7(a) for several members of the rare-earth series. Both the Cu valence and the oxygen content are the same for all these rare-earth elements. No difference in the oxygen uptake has been observed for those rare-earth elements that can exhibit two oxidation states such as Eu or Sm, suggesting that they all substitute as trivalent ions as also deduced from x-ray data. Attempts to lower the oxygen content of these rare-earth phases by annealing them under He or Ar gases at 800°C , using a thermogravimetric apparatus (TGA), did not reveal any oxygen loss greater than 0.1% in weight indicating that as for the undoped phases, the range of non-stoichiometry in oxygen is very narrow, similar to the undoped material. Thus, no further studies have been pursued on the effect of the ambient on the processing of these rare-earth-doped samples.

The superconducting critical temperatures were determined both inductively and resistively and are shown in Fig. 7(b). The variation of the resistivity as a function of temperature from 4.2 to 300 K is shown in Fig. 8 for the Tm-doped 4:3:3:4 samples. The superconducting critical temperature T_c remains constant up to $x=0.5$ and then decreases rapidly so that a semiconducting regime is reached by $x=1.5$ and extending up to $x=2$. The linear

temperature dependence above T_c already observed in most of the superconducting cuprate oxides is still present here.

Note that for the $x=1$ sample the presence of two transitions is indicated and we ascribe this to the presence of stacking faults, as discussed in previous work.²⁴ Such an effect was even more pronounced for the 4:4:2:4 series because of the higher temperatures required for the introduction of the rare-earth element into the compound. The values of T_c (onsets) determined inductively for the members of the 4:3:3:4 and 4:4:2:4 Tm series are shown in Figs. 2(b) and 2(e). The similarity of this figure to that displaying the Cu valence changes [Figs. 2(c) and 2(f)] is striking, supporting the general belief that T_c is related to the amount of Cu III. However, the $x=2$ compound is a

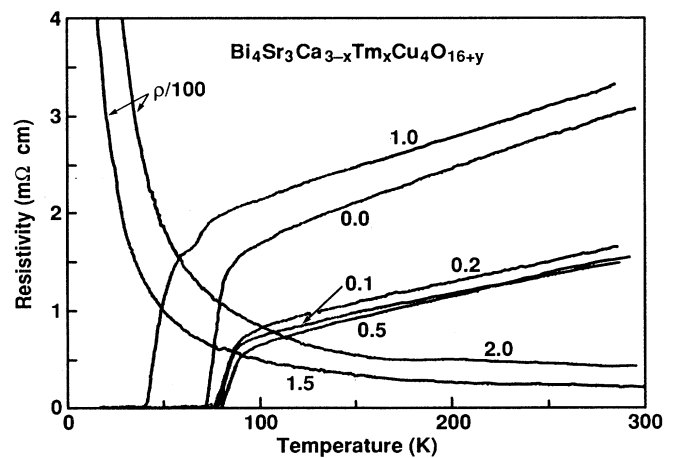


FIG. 7. The resistivity vs temperature from below T_c to room temperature for several members of the $\text{Bi}_4\text{Sr}_3\text{Ca}_{3-x}\text{Tm}_x\text{Cu}_4\text{O}_{16+y}$ series.

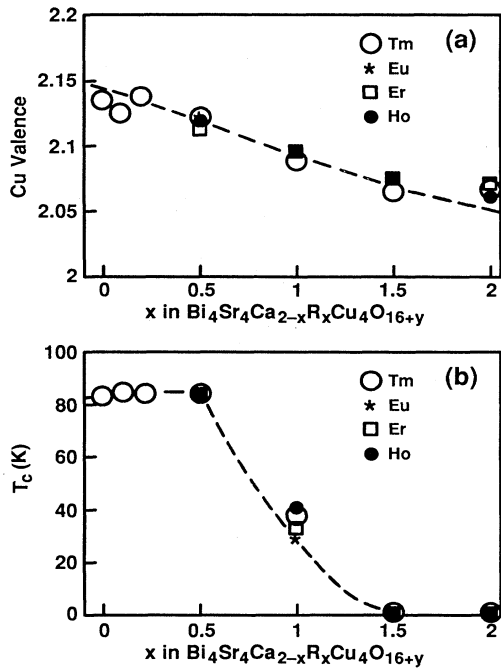


FIG. 8 Effect of the rare-earth substitution on the (a) Cu valence and (b) T_c for several members of the $\text{Bi}_4\text{Sr}_4\text{R}_2\text{Cu}_4\text{O}_y$ series.

semiconductor even with a copper valence greater than 2, suggesting that the correlation between T_c and Cu valence is not a general rule (i.e., the presence of Cu III does not imply superconductivity) or that there is a threshold for the amount of Cu III necessary to obtain a metallic behavior. In Fig. 7 the depression of T_c is shown as a function of x for several rare-earth-doped samples. T_c is depressed in a similar fashion independent of whether the rare-earth

element is magnetic (Er, Tm, Ho), weakly magnetic (Eu), or nonmagnetic (Lu). The data for $R = \text{Lu}$ has not been included in this plot for reason of clarity, since they were identical to those of thulium (see Fig. 2).

Finally, as a direct proof of the oxidation state of the rare-earth ion in these Bi materials, magnetization measurements were performed from 400 K down to 4.2 K in a field of 10 kG using a superconducting quantum interference device (SQUID) magnetometer. The results of these measurements are shown in Fig. 9 where $1/\chi_g$ vs T is plotted for several members of the rare-earth series. The linear variation of $1/\chi_g$ vs T indicates that χ_g changes with temperature in a Curie-Weiss manner. A fit of the data to a Curie-Weiss law of the general formula $\chi_g = C_g / (T + \Theta_p) + \chi_0$ (where C_g , Θ_p , and χ_0 are the Curie constant, the paramagnetic Curie temperature, and the temperature-independent susceptibility, respectively) gives effective magnetic moments for the rare-earth ions close to that expected for free trivalent ions (Table I). The values of Θ_p deduced from the above fit are reported in Table I and compared with Θ_p values obtained for the 1:2:3 materials³² (inset, Fig. 9). From this similarity, and analogous to the $\text{GdBa}_2\text{Cu}_3\text{O}_{7-x}$ phase, one might expect the Gd-doped Bi phase to display magnetic ordering at low temperatures. The magnetic measurements were extended down to 1.7 K on several Gd samples processed differently (i.e., at various annealing temperatures or quenching rates). However, no evidence for magnetic ordering was observed.

For the Nd and Pr-doped samples, the fits of the temperature-dependent susceptibility to a Curie-Weiss law is poorer than those obtained with the other rare-earth elements over the same range of temperature, as indicated by the larger values of the root-mean-square deviation given in Table I. This is due to the slight curvature of $1/\chi$ curves observed for the Nd and Pr samples. Such a deviation from a Curie-Weiss law may result from a crystal-

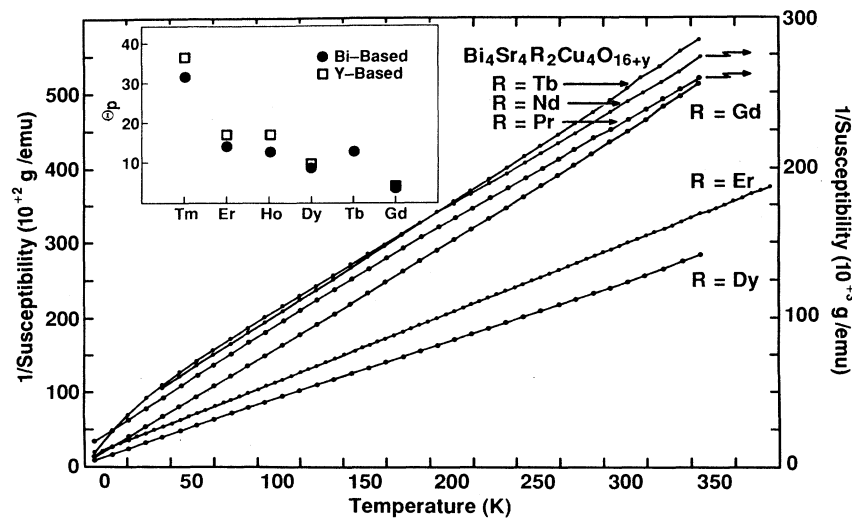


FIG. 9. Magnetization of several members of the $\text{Bi}_4\text{Sr}_4\text{R}_2\text{Cu}_4\text{O}_y$ series measured in a field of 10 kG over the range of temperature 1.7–400 K. The inverse susceptibility temperature dependence is shown. The left scale is for the Nd and Pr samples. The inset compares the Θ_p values for the rare-earth doped $\text{RBa}_2\text{Cu}_3\text{O}_y$ and $\text{Bi}_4\text{Sr}_4\text{R}_2\text{Cu}_4\text{O}_y$ materials.

TABLE I. Lattice parameters for the $\text{Bi}_4\text{Sr}_4\text{R}_2\text{Cu}_4\text{O}_y$ series along with the oxygen content (as determined by chemical analysis). Also reported are the parameters obtained from a fit to a Curie-Weiss law. Shown are the paramagnetic Curie temperature (Θ_p), the effective magnetic moment per M atom (μ_{eff}), and the root-mean-square deviation (rms deviation σ) from the Curie-Weiss law, in percent. Magnetic measurements were collected at a field of 10 kG and the Curie-Weiss fit was performed over the temperature range 50–400 K. The letters vV refer to a van Vleck ion and the (*) indicate that the measurements have not been performed because of material problems.

R	a (Å)	c (Å)	V (Å ³)	Θ_p (K)	μ_{eff} (theory)	μ_{eff} (expt)	σ	Cu III (per unit cell)
La	3.8754	30.592	459.4	*	*	*	*	*
Pr	3.8773	30.366	456.5	16	3.55	2.96	0.03	0.23
Nd	3.8723	30.287	454.2	30	3.55	2.97	0.04	0.15
Sm	3.8673	30.296	453.1	vV	vV	vV	vV	0.20
Eu	3.8630	30.138	449.7	vV	vV	vV	vV	0.15
Gd	3.8550	30.248	449.2	2	7.94	7.84	0.003	0.30
Dy	2.8527	30.162	447.7	8	10.65	10.23	0.003	0.25
Y	3.8530	30.152	447.6	*	0	0.5/Cu	*	0.22
Tb	3.8496	30.232	448.0	13	7.59	7.66	0.002	*
Ho	3.8432	30.025	443.5	13	10.61	10.23	0.002	0.22
Er	3.8412	30.156	444.9	14	9.58	9.39	0.001	0.24
Tm	3.8241	30.173	441.2	32	7.56	7.66	0.002	0.26
Yb	3.8496	30.474	451.6	*	*	*	*	*
Lu	3.8116	30.316	440.4	*	*	*	*	*

field effect at the Nd or Pr site, large enough to lift the degeneracy of the ground state.

Figure 10 displays the susceptibility temperature dependence for both Eu- and Sm-doped Bi samples. Neither follows a Curie-Weiss law as observed for the Gd-doped Bi sample. For the Eu phase the susceptibility increases slightly with decreasing temperature, levels off around 100 K, and increases in a Curie-Weiss manner for temperatures below 50 K. The low-temperature part, most likely due to magnetic impurities, can be corrected as follows: Below 50 K the data were fitted to a Curie-Weiss law so that C_g and Θ_p can be defined. Then over

the temperature-range investigated, we assumed C_g and Θ_p to remain constant and we plotted $\chi = \chi_g - C/(T + \Theta_p)$ to produce the solid curve in Fig. 10. The corrected susceptibility temperature dependence for the Eu-doped Bi sample is similar to that calculated for the van Vleck ion Eu^{+3} ($J=0$), assuming an energy separation of 420 K between the ground state and the first excited state. For the Sm-doped sample the susceptibility temperature dependence does not change in a Curie-Weiss manner, but it is in fair agreement with that expected for the van Vleck ion Sm^{+3} ($J = \frac{5}{2}$) assuming 550 K as separation between the ground state and the first excited state. Thus, magnetic data unambiguously indicate that Eu and Sm are trivalent as already suggested from our x-ray results.

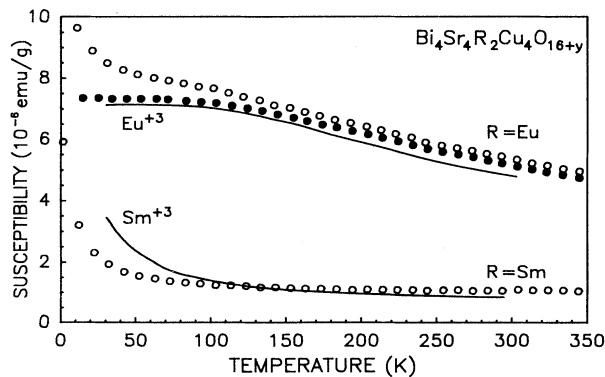


FIG. 10. Magnetic susceptibility, measured in 10 kG, as a function of temperature for $\text{Bi}_4\text{Sr}_4\text{R}_2\text{Cu}_4\text{O}_y$ compounds with $R = \text{Sm}$ and Eu . The observed magnetic susceptibility (open circles) are shown for both phases. The solid line shows the susceptibility for Eu when the Curie contribution has been subtracted out. The solid lines are those expected for free Eu^{3+} ($J=0$) and Sm^{3+} ($J = \frac{5}{2}$) van Vleck ions.

B. Substitution of Sr by R

Samples of general formula $\text{Bi}_4\text{Sr}_{3-x}\text{La}_x\text{Ca}_3\text{Cu}_4\text{O}_{16+y}$ were prepared at 840°C. The x-ray powder-diffraction patterns of the resulting materials indicate that they are multiphase, containing Bragg peaks reminiscent of the $n=1$ Bi-phase and peaks of an unknown phase. The Bragg peaks of the $n=1$ phase, compared to those of the unknown phase, increased their intensity with x and were not exactly located at the same positions as those of the pure $\text{Bi}_2\text{Sr}_2\text{CuO}_y$ phase, suggesting that La may also substitute for Sr in the $\text{Bi}_2\text{Sr}_2\text{CuO}_y$ (2:2:0:1) phase. We thus attempted to prepare the $\text{Bi}_2\text{RCaCuO}_y$ series and succeeded in making single-phase material with $R = \text{La}$, Pr , and Nd at temperatures ranging from 840 to 890°C, in agreement with a previous report by J. Darriet *et al.*³⁰ with $R = \text{La}$. With Sm , the samples were always multiphase, with, however, the $n=1$ phase as the major phase. For the heaviest rare-earth elements, the $\text{Bi}_2\text{RCaCuO}_{6+y}$

TABLE II. The crystal data along with the oxygen content determined by TGA measurements is reported for the $\text{Bi}_2R\text{-CaCuO}_y$ and the $\text{Bi}_2\text{Sr}_2\text{Cu}_{1-x}M_x\text{O}_y$ ($M = \text{Co, Fe}$). The (*) indicates that measurements were not performed.

R	$\text{Bi}_2R\text{CaCuO}_y$			Oxygen content (y)
	$A = \text{\AA}$	$C = \text{\AA}$	$V = \text{\AA}^3$	
Y	5.382	24.51	710.2	6.15
La	5.4068	23.77	695.0	6.6
Pr	5.406	23.65	691.4	6.65
Nd	5.397	23.67	689.5	6.55
Sm	5.383	23.66	685.8	*
Eu to Lu	Phase does not form			*
$\text{Bi}_2\text{Sr}_2\text{Cu}_{1-x}M_x\text{O}_y$				
$M = \text{Co}$				
$x = 0.5$	5.401	24.15	705.4	6.26
$x = 1$	5.445	23.55	698.5	6.53
$M = \text{Fe}$				
$x = 0.5$	5.420	23.92	703.11	6.27
$x = 1$	Multiphase			*

phase did not form. The temperature range at which the phase forms is very narrow, so that annealing temperatures differed from sample to sample, again with the highest temperature (i.e., 920°C) for the lightest rare earth. The crystal data are summarized in Table II. As usually observed, the unit-cell volume increases with increasing ionic radius of the rare earth.

The replacement of two divalent Sr ions by one divalent Ca and one trivalent R modifies the charge balance so that upon substitution, additional oxygen is needed for the structure. Analysis of the resulting material for oxygen either by TGA measurements (Fig. 6), or by chemical titration indeed indicates that upon substitution the oxygen content rises from 6 to 6.5 so that for each added R half an oxygen atom is again added to the structure. Resistivity measurements have shown that the fully substituted compounds are semiconducting even though they contain a small amount of Cu III, as determined by chemical analysis.

Within the $\text{Bi}_2\text{Sr}_2\text{CuO}_y$ phase, two Sr atoms can be replaced by one Ca and one R ion, both of smaller ionic radius than Sr. It might be coincidental but it is exactly when the ionic radius of the rare earth becomes equal to that of Ca or smaller that the phase cannot be formed, stressing again the importance of the steric factors.

C. Substitution within the CuO_2 planes

Our attempts to prepare a pure 85-K phase with Cu substituted or partially substituted by $M = \text{Fe, Co, Al, Ni}$ failed, independent of annealing time and temperature, cooling rates and starting composition (4:4:2:4 or 4:3:3:4). With Al, Ni, and Zn, the (2:2:0:1) phase was present as a trace. A general remark is that no changes in the position of the Bragg peaks of the 85-K phase was observed, suggesting that the substitution of Cu by $3d$ metals and Al does not occur in these materials in contrast to the 40- or

90-K phases. However, in the case of Fe and Co substitutions only, the x-ray pattern contained an increasing amount of the " $\text{Bi}_2\text{Sr}_2\text{CuO}_y$ " peaks with increasing cation substitution. Those Bragg peaks corresponding to the $n = 1$ phase were shifted with respect to those of pure $\text{Bi}_2\text{Sr}_2\text{CuO}_6$, suggesting the ability to substitute Cu by Co or Fe within this phase. We indeed succeeded in preparing compounds of general formula $\text{Bi}_2\text{Sr}_2\text{Cu}_{1-x}M_x\text{O}_y$ with $M = \text{Fe}$ up to 0.5 and Co up to $x = 1$, while we failed with Zn, Al, and Ni.

The crystal data together with the copper valence and oxygen content (as determined chemically and by TGA) are reported in Table II. The unsubstituted 2:2:0:1 is metallic and superconducts at 10 K. The replacement of Cu by Co or Fe induces an uptake of oxygen atoms (0.5 atom for each added Co) suggesting that the valence state of Co is +3. In order to determine the oxidation state of Co in this compound, XPS measurements were also performed. From the position of the Co $2p_{3/2}$ peak located at 781.0 eV it was shown that Co is mostly in the +3 state. The presence of a satellite at 787.1 eV can be ascribed to the high-spin configuration as observed in other Co oxides.³³ Similar measurements with the Co-doped 90-K phase were not possible because of the overlapping of peaks related to Ba and Co.

The magnetic behavior for these Fe- or Co-doped materials is shown in Fig. 11. A prominent feature is the presence of an antiferromagnetic ordering at 140 K for the fully Co-doped sample (Fig. 11). By lowering the cobalt concentration to $x = 0.5$, evidence for antiferromagnetic ordering vanishes. No cusp is observed anymore in the χ vs T curve at low temperature but only a trend of the susceptibility to saturate. The fit to a Curie-Weiss law of the high-temperature part of the curve ($T > 200$ K) gave the parameters $\Theta_p = +3$ K, $\mu_{\text{eff}} = 3.7\mu_B$ per Co atom. This magnetic moment is of the same order as that obtained for Co when substituted for Cu in the $\text{YBa}_2\text{Cu}_{3-x}\text{Co}_x\text{O}_7$ phase ($3.5\mu_B$ per Co) and for which it has been shown that Co is trivalent. This is consistent with the XPS interpretation. For the iron sample of intermediate composition ($\text{Bi}_2\text{Sr}_2\text{Cu}_{0.5}\text{Fe}_{0.5}\text{O}_{6.25}$), we also observe a leveling off of the susceptibility at low temperature, same as for the $\text{Co}_{0.5}$ doped sample, but no satisfactory Curie-Weiss fit could be obtained at higher temperature. The relationship between structural, magnetic, and electrical properties for these samples will be described elsewhere.

At this point an interesting comparison can be made with the 90-K system for which it has been shown that Cu can be substituted by $3d$ metals, with the trivalent ones (Co, Al, and Fe) going onto the chains (where they end up octahedrally coordinated) and the divalent ones replacing Cu within the planes. But the divalent ions cannot be substituted for Cu in the 2:2:0:1 Bi phase whereas Co and Fe can. The main reason for the inability to substitute Cu and Fe for Cu within the 4:4:2:4 phase, while this substitution succeeds in the 2:2:0:1 phase may arise from the fact that Cu is fivefold coordinated in the first one while it is sixfold coordinated in the second one. This is consistent with our previous findings on the 90-K material that Co was not going on the CuO_2 planes (Cu fivefold coordinat-

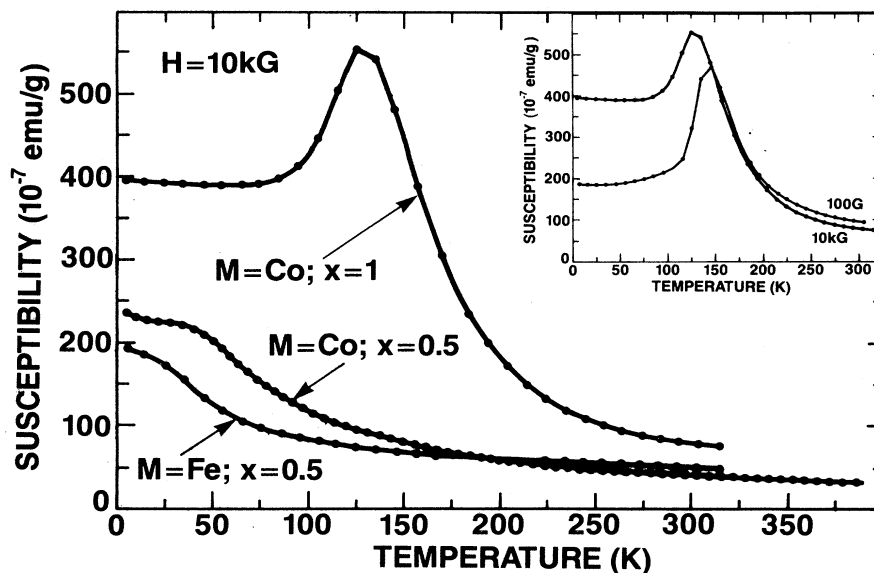


FIG. 11. The observed susceptibility temperature dependence is shown for members of the $\text{Bi}_2\text{Sr}_2\text{Cu}_{1-x}\text{M}_x\text{O}_y$ series. When $M = \text{Co}$, the data are shown for the compositions $x = 0.5$ and 1 and for when $M = \text{Fe}$ for $x = 0.5$. The inset shows the effect of the applied magnetic field on the magnetic transition.

ed) but on the chains dragging extra oxygen atoms to become sixfold coordinated. However, following the same line of reasoning, the Cu coordination within the CuO_2 plane of the Y-based superconductor is similar to the 85-K Bi-based oxide and one should expect the Ni substitution to work for the Bi phase, contrary to what we observe experimentally.

III. DISCUSSION

A. 4:4:2:4 composition

Some doubts still persisted about the ideal structural 4:4:2:4 composition deduced from single-crystal x-ray studies on the 85-K Bi-phase ($n = 2$) since, for instance, the existence of a solid solution implies that some of the Ca ions occupy the Sr sites (denoted as S). A recent synthesis and crystal-structure study of the $\text{Ca}_{0.85}\text{Sr}_{0.15}\text{CuO}_2$ also indicates that Sr in a small amount, may also occupy the C sites.³⁴ Thus, we have the possibility of Sr substitution on the C sites and vice versa. The study of the $\text{Bi}_4\text{Sr}_3\text{Ca}_{3-x}\text{R}_x\text{Cu}_4\text{O}_{16+y}$ system has shown that Ca can be substituted by Tm whereas Sr cannot be substituted at all by a R [or $(\text{Ca} + R)/2$ as for the 2:2:0:1 phase]. Moreover the maximum substitution for calcium is $x = 2$ which is the number of C sites. This cationic substitution supports the ideal structural composition $\text{Bi}_4\text{S}_4\text{C}_2\text{Cu}_4\text{O}_{16}$ with the majority of the C sites occupied by Ca, while the S site can actually be a mixture of Sr and Ca.

B. Oxygen stoichiometry

The substitution of Ca by a R within the $\text{Bi}_4\text{Sr}_4\text{-Ca}_{2-x}\text{R}_x\text{Cu}_4\text{O}_{16+y/2+y}$ system theoretically induces the uptake of half an oxygen atom per substituted Ca if the Cu valence is assumed to be constant. This is true when

the amount of the substitution is less than $x = 1$. Beyond this value, the oxygen uptake does not follow the substitution. This is accommodated by a decrease in the formal Cu valence and a vanishing of the superconducting properties. The location of the extra oxygen in the structure remains the key question. By analogy to the $\text{YBa}_2\text{Cu}_3\text{O}_7$ phase, it is unlikely that oxygen goes within the R planes. However, within the 85-K Bi structure, due to the quite long spacing between the Bi-O layers, there are sites that can geometrically accommodate as many as two extra oxygen atoms per formula unit.⁸ There is also the possibility of the existence of BiO_{1+x} layers (i.e., extra oxygen atoms within the layers). Single-crystal x-ray studies and more importantly, neutron-diffraction measurements, should succeed in locating within the structure the 1.5 extra oxygen atoms per formula unit in the R -doped materials.

C. Modulation

HREM studies have shown that the incommensurate modulation of the structure is still present in the Tm-substituted samples. The propagation vector is slightly smaller (4.3*b*) than in the undoped material (4.7*b*). Since the oxygen stoichiometry differs by 1 between these two samples, the presence of this modulation in both samples indicates that the modulation does not correlate strongly with oxygen defects. This confirms previous work associating the modulation with Bi atoms moving within and out of their planes.^{26,27} As shown by Gao *et al.*,²⁷ every 4.7 (i.e., ~ 5) cell unit there are 2 Bi atoms moving closer together so that the spacing between the Bi layers is not uniform but modulated with narrowed and enlarged sections (i.e., pockets, see Fig. 2 of Ref. 27). By adding extra oxygen atoms in these vacant sites between the Bi planes one forms "Aurevillius-type" phase blocks which coexist with the NaCl-type blocks of these Bi-O layers.

The formation of an Aurevillius block (i.e., short Bi-O bonds) might imply the formation of Bi^{5+} . But within the enlargement zones created by the modulation, Bi-O bonds of reasonable length can be formed so that they are consistent with Bi remaining +3. This is consistent with XPS studies on the Er substituted ($x=2$) phase that does not show any Bi^{5+} .

Since the modulation repeats approximately every 5 Bi atoms, enlarging 3 Bi-O bonds, only $\frac{2}{5}$ to $\frac{3}{5}$ (roughly) of the two sites (i.e., 0.8 to 1.2 site per 4:4:2:4 formula unit) available per unit cell will accommodate an extra oxygen. This may explain why at low substitutions each rare-earth element may drag in half an extra oxygen while the oxygen uptake slows down at higher substitutions.

A similar modulation exists for the 2:2:0:1 phase. Substitutions in this compound have shown that only one La (and 0.5 oxygen atoms) can be inserted. Attempts to introduce 2 La (and 1 oxygen atom) fails. Since La has an ionic radius similar to Sr, steric factors cannot account for such a failure. Similar to the 2:2:2:3 phase the replacement of Ca by R will also introduce one oxygen. In both cases the rare-earth substitution will require the uptake of one oxygen but the structure can only accommodate 0.5. Thus, the compound does not form. This interpretation is at least consistent with the experimental observations.

D. Cu valence

Similar to the $\text{La}_{2-x}\text{Sr}_x\text{CuO}_4$ system and other systems, we find that changes in T_c are correlated to changes in Cu III (i.e., hole concentration). However, in the nonsuperconducting regime there is still some Cu III. The $\text{Bi}_2\text{RCaCuO}_6$ phases reported herein contain around 0.1 Cu III per formula unit. However, they are semiconducting. This indicates that just the presence of Cu III does not systematically imply superconducting behavior.

An interesting comparison can be made with the $\text{Y}_{1-x}\text{R}_x\text{Ba}_2\text{Cu}_3\text{O}_y$ system where upon increasing the rare-earth content (x), T_c does not change. In both phases the rare-earth atoms occupy identical sites, but the main difference resides in the fact that for the Bi phase the addition of extra oxygen is required to keep the Cu valence constant. These substitutions do not affect T_c as long as the Cu valence remains constant. Beyond a limit, where oxygen uptake is insufficient to compensate, the rare-earth substitution leads to a change in the number of holes while for the 90-K phase the amount of oxygen (i.e., the number of holes or Cu III) does remain constant through the range of substitution. This is further indication that among these cuprate oxides, the T_c 's are extremely sensitive to chemical substitutions affecting the hole concentration. Similar to the rare-earth-doped 90-K series, we find for the rare-earth-Bi phases that T_c is independent of whether the substituted rare-earth element is magnetic or nonmagnetic.

E. Magnetic properties

We succeeded in synthesizing a semiconducting parent compound of the 85-K Bi phase. Thus analogous to the

40- or 90-K phase one would expect these materials to show evidence for antiferromagnetic ordering associated with the Cu ions. But, the detection of this ordering by magnetic measurements might be hindered by the large magnetic moments of the rare-earth elements, with the exception of Eu and Sm samples, for which the susceptibility is small (La and Lu were excluded because the samples were multiphase). However, neither the Eu nor Sm sample shows detectable anomalies in the susceptibility up to 400 K, indicating that there is no long-range magnetic ordering transition in these compounds over this temperature range. Neutron experiments have been done on the $\text{Bi}_4\text{Sr}_4\text{Y}_2\text{Cu}_4\text{O}_y$ sample and no magnetic reflections corresponding to magnetic ordering have been detected.³⁵ This result agrees with our magnetic data, but is in contrast with muon-spin-resonance studies³⁶ which show the existence of magnetism in semiconducting $\text{Bi}_4\text{Sr}_4\text{Y}_2\text{Cu}_4\text{O}_y$ compound for temperatures lower than 300 K. It is also worthwhile to mention that by muon-spin resonance, the coexistence of magnetism and superconductivity has been found within the Co-doped $\text{YBa}_2\text{Cu}_{3-x}\text{Co}_x\text{O}_y$ series ($0 < x < 0.2$),³⁶ but neutron-diffraction studies failed to confirm this point.³⁷ Muon-spin resonance is sensitive to local magnetic interactions whereas neutrons are sensitive to long-range magnetic order. Thus sample inhomogeneities might be the origin of these observed differences. Thus the existence of antiferromagnetism within the semiconducting parent $\text{Bi}_2\text{Sr}_2\text{RCu}_2\text{O}_y$ phase still remains an important dilemma.

IV. SUMMARY

We have shown that the cationic substitution within the Bi system has led to new compounds such as $\text{Bi}_4\text{Sr}_4\text{R}_2\text{Cu}_4\text{O}_y$, $\text{Bi}_2\text{RCaCuO}_y$, or $\text{Bi}_2\text{Sr}_2\text{Cu}_{1-x}\text{M}_x\text{O}_y$. From structural and physical property studies we presented evidence that the 4:4:2:4 phase is indeed the structural composition of the 85-K Bi phase and showed that its structural modulation is not related to the oxygen content. We found that the superconducting properties of the substituted 85-K material are independent of the dopant whether it is magnetic or nonmagnetic, but these properties are strongly affected by changes in the hole concentration induced by the amount of doping. Like the Cu-O chains for the 90-K material, the double Bi-O layer acts as oxygen reservoirs for the Bi phases. Any modification of this double Bi layer (through uptake of oxygen) affects the hole concentration and thereby drastically affects T_c . There are still unanswered questions, such as whether antiferromagnetism exists at temperatures higher than 400 K for the semiconducting $\text{Bi}_4\text{Sr}_4\text{R}_2\text{Cu}_4\text{O}_y$ phase and where the extra oxygens are located in the structure (within or without the BiO layers). Further work presently in progress should answer these questions.

ACKNOWLEDGMENTS

We wish to thank B. G. Bagley, B. Chevalier, J. Darrriet, P. L. Key, Y. LePage, P. Miceli, J. M. Rowell, G. Thomas, and J. H. Wernick for helpful discussions.

- ¹J. M. Tarascon, L. H. Greene, W. R. McKinnon, G. W. Hull, and T. H. Geballe, *Science* **235**, 1373 (1987).
- ²M. W. Shafer, T. Penney, and B. L. Olson, *Phys. Rev. B* **36**, 4047 (1987).
- ³J. B. Torrance, Y. Tobura, A. J. Nazzari, A. Bezing, T. C. Huang, and S. S. P. Parkin, *Phys. Rev. Lett.* **61**, 1127 (1988).
- ⁴N. P. Ong, Z. Z. Wang, J. Clayhold, J. M. Tarascon, L. H. Greene, and W. R. McKinnon, *Phys. Rev. B* **35**, 8807 (1987).
- ⁵P. K. Gallagher, H. M. O'Bryan, S. A. Sunshine, and D. W. Murphy, *Mater. Res. Bull.* **22**, 995 (1987).
- ⁶J. D. Jorgensen, M. A. Beno, D. G. Hinks, L. Soderholm, K. J. Volin, R. L. Hitterman, J. D. Grace, I. K. Schuller, C. U. Segre, K. Zhang, and M. S. Kleefish, *Phys. Rev. B* **36**, 3608 (1987).
- ⁷H. Maeda, Y. Tanaka, M. Fukusutomi, and T. Asano, *Jpn. J. Appl. Phys.* **27**, L209 (1988).
- ⁸J. M. Tarascon, Y. LePage, P. Barboux, B. G. Bagley, L. H. Greene, W. R. McKinnon, G. W. Hull, M. Giroud, and D. M. Hwang, *Phys. Rev. B* **37**, 9382 (1988).
- ⁹S. Sunshine, T. Siegrist, L. F. Schneemeyer, D. W. Murphy, R. J. Cava, R. B. van Dover, R. M. Fleming, S. H. Glarum, S. Nakahara, R. Farrow, J. J. Krajewski, S. M. Zahurak, J. V. Waszczak, J. H. Marshall, P. Marsh, L. W. Rupp, Jr., and W. F. Peck, *Phys. Rev. B* **38**, 893 (1988).
- ¹⁰M. A. Subramanian, C. C. Torardi, J. C. Calabrese, J. Gopalakrishnan, K. J. Morissey, T. R. Askew, R. B. Flippen, U. Chowdry, and A. W. Sleight, *Science* **239**, 1015 (1988).
- ¹¹Z. Z. Sheng and A. M. Hermann, *Nature* **332**, 55 (1988); **332**, 138 (1988).
- ¹²D. Vaknin, S. K. Sinha, D. E. Moncton, D. C. Johnston, J. Newman, C. R. Safinya, and H. E. King, Jr., *Phys. Rev. Lett.* **58**, 2802 (1987).
- ¹³J. M. Tranquada, D. E. Cox, W. Kunmann, H. Moudden, G. Shirane, M. Suenaga, P. Zolliker, D. Vaknin, S. K. Sinha, M. S. Alvarez, A. J. Jacobson, and D. C. Johnston, *Phys. Rev. Lett.* **60**, 156 (1988).
- ¹⁴P. W. Anderson, G. Baskaran, Z. Zou, and T. Hsu, *Phys. Rev. Lett.* **58**, 2790 (1987).
- ¹⁵V. J. Emery, *Phys. Rev. Lett.* **58**, 2794 (1987).
- ¹⁶J. E. Hirsch, *Phys. Rev. Lett.* **59**, 228 (1987).
- ¹⁷J. M. Tarascon, L. H. Greene, P. Barboux, W. R. McKinnon, G. W. Hull, T. P. Orlando, K. A. Delin, S. Foner, and E. J. McNiff, *Phys. Rev. B* **36**, 8393 (1987).
- ¹⁸Y. Maeno, T. Tomita, M. Kyogoku, S. Awaji, Y. A. Oki, K. Oshino, A. A. Minami, and T. Fujita, *Nature* **328**, 512 (1987).
- ¹⁹G. Xiao, F. H. Streitz, A. Gavrin, Y. W. Du, and C. L. Chien, *Phys. Rev. B* **35**, 8782 (1987).
- ²⁰J. M. Tarascon, P. Barboux, P. F. Miceli, L. H. Greene, and G. W. Hull, *Phys. Rev. B* **37**, 7458 (1988).
- ²¹C. Michel, M. Hervieu, M. M. Borel, A. Grandin, F. Deslandes, J. Provost, and B. Raveau, *Z. Phys. B* **68**, 421 (1987).
- ²²C. C. Torardi, M. A. Subramanian, J. C. Calabrese, J. Gopalakrishnan, K. J. Morissey, T. R. Askew, R. B. Flippen, U. Chowdry, and A. W. Sleight, *Phys. Rev. B* **38**, 225 (1988).
- ²³J. M. Tarascon, Y. LePage, L. H. Greene, B. G. Bagley, P. Barboux, D. M. Hwang, G. W. Hull, W. R. McKinnon, and M. Giroud, *Phys. Rev. B* **38**, 2504 (1988).
- ²⁴J. M. Tarascon, W. R. McKinnon, P. Barboux, D. M. Hwang, B. G. Bagley, L. H. Greene, G. W. Hull, Y. LePage, N. Stoffel, and M. Giroud, *Phys. Rev. B* **38**, 8885 (1988).
- ²⁵G. S. Gruder, E. M. Gyorgy, P. K. Gallagher, H. M. O'Bryan, D. W. Johnson, S. Sunshine, S. M. Zahurak, S. Jin, and R. C. Sherwood, *Phys. Rev. B* **38**, 757 (1988).
- ²⁶E. A. Hewatt, P. Bordet, J. J. Caponi, C. Chaillet, J. L. Hodeau, and M. Marezio, *Physica C* **153-155**, 619 (1988).
- ²⁷Y. Gao, P. Lee, P. Coppens, M. A. Subramanian, and A. W. Sleight, *Science* **241**, 954 (1988).
- ²⁸A. Manthiram and J. B. Goodenough, *Appl. Phys. Lett.* **53**, 420 (1988).
- ²⁹B. Chevalier, B. Lepine, A. LeLirzin, J. Darriet, J. Etourneau, and J. M. Tarascon, *Mat. Sci. Eng.* (to be published).
- ³⁰J. Darriet, B. Lepine, A. LeLirzin, B. Chevalier, and J. Etourneau (unpublished).
- ³¹J. M. Tarascon, L. H. Greene, B. G. Bagley, W. R. McKinnon, P. Barboux, and G. W. Hull, in *Novel Superconductivity*, edited by S. A. Wolf and V. Z. Kresin (Plenum, New York, 1987), p. 705.
- ³²J. M. Tarascon, W. R. McKinnon, L. H. Greene, G. W. Hull, and E. M. Vogel, *Phys. Rev. B* **36**, 226 (1987).
- ³³C. N. R. Rao, D. D. Sarma, S. Vasudevan, and M. S. Hegde, *Proc. R. Soc. London, Ser. A* **367**, 239 (1979).
- ³⁴T. Siegrist, S. M. Zahurak, D. W. Murphy, and B. S. Roth, *Nature (London)* **337**, 231 (1988).
- ³⁵P. F. Miceli *et al.* (unpublished).
- ³⁶Y. J. Uemera, B. J. Sternlieb, D. E. Cox, V. J. Emery, A. Moodenbaugh, and M. Suenaga, *J. Phys. (Paris)* (to be published).
- ³⁷P. F. Miceli, J. M. Tarascon, L. H. Greene, P. Barboux, M. Giroud, D. A. Neumann, J. J. Rhyne, L. F. Schneemeyer, and J. V. Waszczak, *Phys. Rev. B* **38**, 9209 (1988).

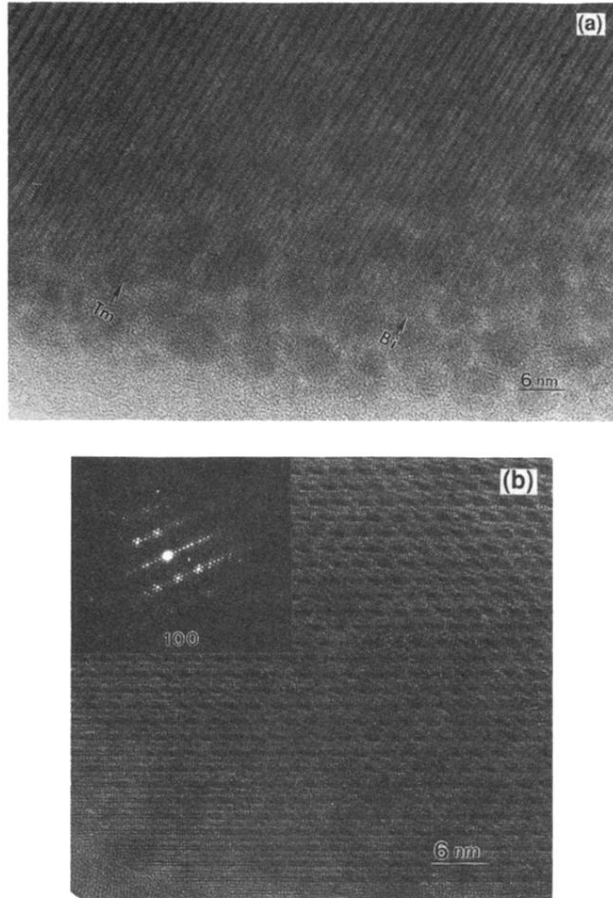


FIG. 3. High resolution electron microscopy image (a) in the [010] zone axis showing the Bi layers and the prominent Tm layers (arrowed). (b) In the [100] zone axis showing the modulated structure similar to that in undoped $\text{Bi}_4\text{Sr}_4\text{Ca}_2\text{Cu}_4\text{O}_{16}$ samples. Inset shows the [100] selected area diffraction pattern.